Investigation of Multi-Band Microwave Filters Using a Corrugated Rectangular Waveguide

Issa W. Al-Hmoud[a], Mohammed H. Bataineh[b]

Department of Telecommunications Engineering, Yarmouk University, Irbid, Jordan
[a]e-mail: issawalhmoud91@gmail.com
[b]e-mail: mohbat@yu.edu.jo

Abstract— In this paper, filtering characteristics of guided waves in a rectangular waveguide with corrugations on the side walls are investigated. The parameters of the sidewalls offer an added degree of freedom to the filter designer for controlling the width of the stopband region. A rectangular waveguide with sinusoidal and square corrugations, that are uniform along the structure depth, is simulated using two commercial full-wave solvers, the HFSS and CST Studio Suite. However, the frequency response for a uniform waveguide with sinusoidal corrugation has the undesirable effect of high ripple levels, which corrupts the filter response without a clear isolation between stop-band and pass-bands. Apodization profile is introduced to decrease the level of the ripples. The Gaussian apodization profile has been examined. The square corrugation profile has been used to investigate the multi-bands in the frequency response.

Keywords— Apodization profile, CST, HFSS, inverted notch filter, level of the ripples, microwave filters, periodic structure.

I.   INTRODUCTION

Waveguides with a periodic structure are commonly used as wave filters and couplers in various applications. Periodic structures are built in the waveguide to transfer their function from a device that merely guides and/or confines the electromagnetic waves at microwave frequencies, to that which can be used as a filter or a coupler, or even a mode converter. Such waveguides with periodic structures are called corrugated waveguides; and they can be of different types and shapes.

Corrugated waveguides can be used as a microwave filter due to the constructive and destructive behavior of the wave propagating within the guide. The corrugation could be either uniform or non-uniform; and it could be of different shapes like sinusoidal or square corrugations.

The filtering characteristics of corrugated waveguides can be adjusted by changing the design of the unit cell that is repeated and joined together to form the whole structure.

The design of the unit cell that forms the periodic structure identifies the filtering properties of the structure. Therefore, transmission properties of the waveguide can be altered by changing the corrugation profile.

The perturbation method of multiple scales [1], [2] was used by many researchers to analyze the propagation of waves in both bounded and unbounded waveguides with different corrugation profiles [3]-[10]. The analysis of wave propagation in corrugated waveguides using the perturbation technique leads to a system of coupled-mode ordinary differential equation that may be solved numerically or sometimes analytically to calculate the filter response.

In [11]-[13], different approaches have been used to handle the filtering characteristics of corrugated waveguides. In [11], a novel way, asymptotic corrugations boundary conditions

"ACBC", is used to solve all-four walls axially corrugated rectangular waveguides. This method considers two linear systems of equations: one pertains to the ACBCs of the left and right corrugated walls; the other is associated with those of the upper and lower corrugated walls before combining them. In [12], a band-pass filter using an improved structure of rectangular waveguide is proposed. The filter consists of cascade resonant cavities, each of different width to broaden the suppression of the stop-band region. In [13], a simple quasi-analytical method to design classical corrugated rectangular waveguide low pass filters is presented. The proposed method gives a final closed form expression for the filter dimension. The filtering characteristics of corrugated waveguides are due to the Bragg reflection phenomenon. Bragg reflection is a consequence of cumulative reflections in the periodic structure leading to the presence of a forbidden gap in the electromagnetic spectrum [14], [15]. Hence, it is natural to find stop-bands, pass-bands and band-gaps in a periodic structure.

In a waveguide having a sinusoidal periodic corrugation, the stop-band occurs above the cutoff of each mode. These stop-bands are characterized by a first-order Bragg condition that couples a forward mode with its reflection. Thus, for TE waves in a parallel-plate waveguide, for instance, the first stop-band appearing above the cutoff corresponds to the reflection of the dominant TE_{10} mode.

The problem of a sinusoidal wall corrugation was treated by Nayfeh and Asfar [3], where the same sinusoidal corrugation existed on both walls of a parallel-plate waveguide. Sinusoidal corrugation is more difficult to manufacture than, for example, a square- wave corrugation. The latter provides extra periods required to realize the higher-order stopbands through the harmonics of the wall corrugation. Harmonics of the square-wave cause higher-order Bragg conditions to be satisfied for all propagating modes.

Simulation for the proposed geometries has been handled using two commercial software packages, Ansoft High Frequency Structure Simulator (HFSS) [16] and CST Microwave Studio Suite [17]. HFSS is based on the Finite Element Method (FEM). FEM is a method based on solving partial differential equations. It subdivides space in elements. Fields inside these elements are expressed in terms of a number of basic functions. These expressions are inserted into the function of the equations; and the variation of the function is made zero. This yields a matrix eigenvalue equation whose solution yields the field at the nodes. FEM normally formulated in the frequency domain. This means that the solution has to be calculated for every frequency of interest. Useful features of HFSS include its automatic adaptive mesh generation and refinement, which in most cases free the designer of worrying about which mesh/grid to choose. The CST Microwave Studio is based on the Finite Integration Technique (FIT). It allows choosing the time domain as well as the frequency domain approach. The flagship module of CST MWS is the transient solver. In this solver, the automatic mesh generator detects important points inside the structure (fixpoints) and locates mesh nodes there. The user can manually add fixpoints on a structure, and fully control the number of mesh lines in each coordinate with regards to the specified wavelength. A problem observed with CST is a ripple in the frequency response in case tool settings are not appropriate; this is due to the fact that the flagship of CST is inherently a time domain solver.

II. FORMULATION

To analyze the problem of interest, one needs to solve the Helmholt'z equation and then apply the boundary conditions. Those boundary conditions are when the tangential components of the electric field equals zero. The propagation of the dominant mode of transverse electric

(TE_{10}) waves in a rectangular waveguide whose lateral walls have different corrugation profiles such as sinusoidal and square undulations is considered in the following subsections.

A) Rectangular Waveguide with Sinusoidal Corrugations Profile

In this section, the TE waves in a rectangular waveguide as shown in Fig. 1 are considered. Surfaces at the right and left walls are assumed to perfectly conduct and have a distortion function of the form
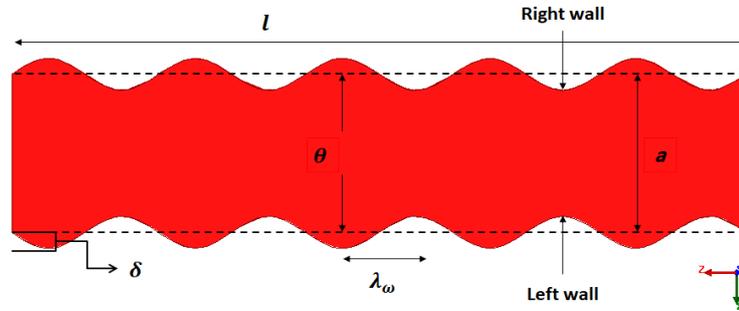

Fig. 1. Top-view for a rectangular waveguide of the sinusoidal wave corrugation

$$\tilde{x} = d_1 sin(\tilde{k}_\omega \tilde{z}) \quad \text{at } \tilde{x} = 0 \tag{1}$$

$$\tilde{x} = a + d_2 sin(\tilde{k}_\omega \tilde{z} + \theta) \quad \text{at } \tilde{x} = a \tag{2}$$

where $\tilde{x}$ and $\tilde{z}$ are dimensional coordinates; d_1 and d_2 are the amplitudes of the sinusoidal corrugation; a is the unperturbed separation of the sides; $\tilde{k}_\omega$ is the wave number of the corrugation; θ is the phase difference between the two corrugated walls; and l is the length of the corrugated section. The coordinate is made dimensionless by choosing the average separation a to normalize all length quantities.

The field component E_y has been selected as a dependent variable using the standard procedure of arranging Maxwell's equations [18]. The governing equation for E_y is given by:

$$\left[\left(\frac{\partial^2}{\partial x^2} + \frac{\partial^2}{\partial z^2}\right) + k_0{}^2\right]E_y = 0 \tag{3}$$

where $k_0 = \omega\sqrt{\mu_0\varepsilon_0}$ is the free space wavenumber. The boundary conditions associated with the governing equation are given by:

$$E_y = 0, \quad \text{at } x = \delta sin(k_\omega z) \tag{4}$$

$$E_y = 0, \quad \text{at } x = 1 + \alpha\delta sin(k_\omega z + \theta) \tag{5}$$

Here, x and z are the dimensionless coordinates; $\delta = \frac{d_1}{a}$ is a dimensionless small parameter; $\alpha = \frac{d_2}{d_1}$ is the ratio between the amplitudes of sinusoidal corrugations.

Following [1], the method of multiple scales can be used to solve (3) subjected to (4) and (5). The core of this method lies in the expansion of E_y in a power series of δ:

$$E_y(x,z) = E_y{}^{(0)}(x,z_0,z_1,z_2) + \delta E_y{}^{(1)}(x,z_0,z_1,z_2) + \delta^2 E_y{}^{(2)}(x,z_0,z_1,z_2)+\dots \tag{6}$$

In accordance with the method of multiple scales $z_0 = z$, $z_1 = \delta z_0$, and $z_2 = \delta^2 z_0$.

Following the procedure described in [19], the system of coupled mode equations of second order in δ that represents the incident and reflected wave amplitudes, u^+ and u^- is given by:

$$\begin{bmatrix} D_z(u^+) \\ D_z(u^-) \end{bmatrix} = \begin{bmatrix} j\delta^2 G_1 & \delta Q_1 \left[1 + \delta\frac{\sigma}{2k}\right] \\ \delta Q_2 \left[1 + \delta\frac{\sigma}{2k}\right] & j\delta[\sigma - \delta G_1] \end{bmatrix} \begin{bmatrix} u^+ \\ u^- \end{bmatrix} \tag{7}$$

The operator D_z stands for the derivative with respect to z. The entries of the system in (7) are given by:

$$Q_1 = -\left(\frac{\pi^2}{2k}\right)\left[1 - \alpha e^{-j\theta}\right] \tag{8}$$

$$Q_2 = -\left(\frac{\pi^2}{2k}\right)\left[1 - \alpha e^{j\theta}\right] \tag{9}$$

$$G_1 = \frac{\pi^2}{4k}\left\{[1 + \alpha^2]\left(\frac{\beta cosh(\beta)}{sinh(\beta)} - 0.5\left(\frac{\pi}{k}\right)^2\right) + 2\alpha cos(\theta)\left(\frac{\beta}{sinh(\beta)} + 0.5\left(\frac{\pi}{k}\right)^2\right)\right\} \tag{10}$$

where k is the propagation constant generally given by $k_{mn} = \sqrt{k_0^2 - (\frac{m\pi}{a})^2 - (\frac{n\pi}{b})^2}$; and σ is a detuning parameter representing the Bragg condition ($k_\omega = 2k$) at the center of the stopband region. This parameter is given by:

$$\sigma = \frac{2k - k_\omega}{\delta} \tag{11}$$

The parameter β is given by $\beta = \sqrt{(k + k_\omega)^2 - k_0^2}$. The system in (7) is subject to the two-point boundary conditions:

$$u^+(0) = 1 \tag{12}$$

$$u^-(l) = 0 \tag{13}$$

Waveguide dimensions have been selected for the waveguide to be operated in the S-band. Therefore, the parameters are

TABLE 1
PARAMETER VALUES FOR THE PROPOSED RECTANGULAR WAVEGUIDE

Parameter	Value	Parameter	Value	Parameter	Value
a	7.5 [cm]	f	3 [GHz]	$k_{10} = \sqrt{(\frac{2\pi f}{c})^2 - (\frac{\pi}{a})^2}$	46.832 [m^{-1}]
$k_\omega = 2k$	93.6641 [m^{-1}]	$\lambda_\omega = \frac{2\pi}{k_\omega}$	6.708 [cm]	$l = 20\lambda_\omega$	134.16 [cm]

Fig. 2 shows an excellent agreement between HFSS and CST for a power reflection coefficient. It can be observed that the frequency response contains only a single stop-band.
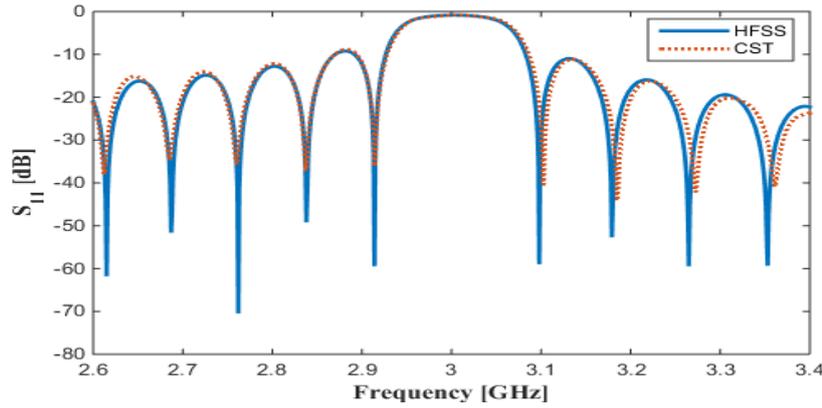
Fig. 2. Reflection coefficient for rectangular waveguide with sinusoidal wave corrugation for α=1, θ=π, and δ=0.03a

A.1. Rectangular waveguide of sinusoidal corrugations profile with phase reverse

In this subsection, a rectangular corrugated waveguide, whose sinusoidal corrugation reverses phase halfway along the waveguide, is investigated [20]. Fig. 3 shows a phase reverse applied at half the structure depth l. This is made by changing the sign of corrugation depth amplitude δ for $l > \frac{l}{2}$. The correspondence system for the case of a single phase reversal is:

$$\begin{bmatrix} D_z(u^+) \\ D_z(u^-) \end{bmatrix} = \begin{bmatrix} 0 & \delta Q_1 \\ \delta Q_2 & j\delta\sigma \end{bmatrix}\begin{bmatrix} u^+ \\ u^- \end{bmatrix}, \ l < \frac{l}{2} \tag{14}$$

$$\begin{bmatrix} D_z(u^+) \\ D_z(u^-) \end{bmatrix} = \begin{bmatrix} 0 & -\delta Q_1 \\ -\delta Q_2 & j\delta\sigma \end{bmatrix}\begin{bmatrix} u^+ \\ u^- \end{bmatrix}, \ l > \frac{l}{2} \tag{15}$$
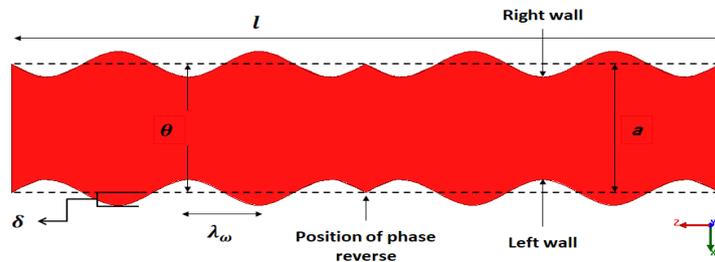

Fig. 3. Top-view for a rectangular waveguide of sinusoidal wave corrugation with phase revers at $\frac{l}{2}$ for α=1, θ=π, and δ=±0.03a

The S_{11} result for this structure is shown in Fig. 4. It can be noted that as a result of reversing the corrugation depth amplitude δ sign, an inverted notch filter, which is a narrow pass-band filter in the region of the stop-band filter region, has been created.
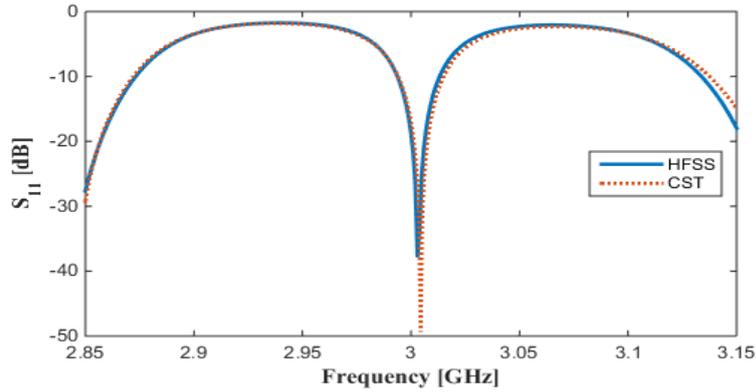
Fig. 4. Reflection coefficient for a rectangular waveguide of sinusoidal wave corrugation with phase reverse at $\frac{l}{2}$ for $\alpha=1$, $\theta=\pi$, and $\delta=\pm0.03a$

A.2.　Rectangular waveguide of non-uniform sinusoidal corrugations with Gaussian apodization profile

The case of non-uniform corrugation can be handled by introducing an apodization profile into the boundary of the uniform corrugated waveguide [21], as suggested in (16) and (17):

$$E_y = 0 \quad \text{at } x = \delta f(z_1)sin(k_\omega z) \tag{16}$$

$$E_y = 0 \quad \text{at } x = 1 + \alpha\delta f(z_1) \, sin(k_\omega z) \tag{17}$$

Following the same procedure in [19] with (16) and (17) considered boundary conditions corresponding to the governing (3), the system that represents the solution of first-order problem would take the form:

$$\begin{bmatrix} D_z(u^+) \\ D_z(u^-) \end{bmatrix} = \begin{bmatrix} 0 & \delta f(z)Q_1 \\ \delta f(z)Q_2 & j\delta\sigma \end{bmatrix} \begin{bmatrix} u^+ \\ u^- \end{bmatrix} \tag{18}$$

The system in (18) corresponds to $u^+(0) = 1$ and $u^-(l) = 0$. In this paper the following apodization profile has been introduced to a rectangular waveguide with sinusoidal corrugation as shown in Fig. 5. The resultant reflection coefficient is shown in Fig. 6.
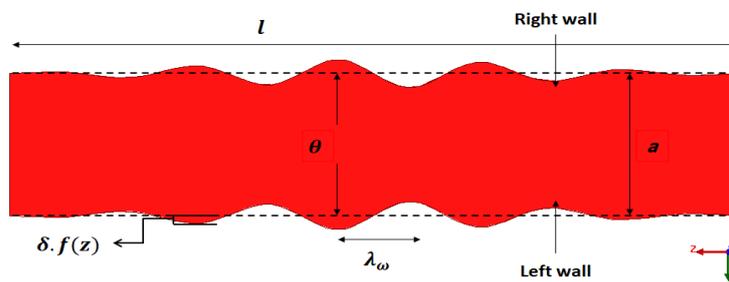

Fig. 5. Top-view for a rectangular waveguide of non-uniform sinusoidal wave corrugation with Gaussian apodization profile

$$f(z) = e^{-c_0((\frac{z}{l}-0.5)^2)} \tag{19}$$

where l is structure depth; and c_0 is an arbitrary constant. Fig. 7 shows a comparison of power reflection coefficient in a uniform and non-uniform rectangular corrugated waveguide. Introducing the apodization profile $f(z)$ has decreased the level of ripples and broadened the bandwidth of the stop-band region. A small drop in the amplitude of S_{11} can be observed. The drop could result from decrement in the amplitude of the corrugation depth δ which multiplying by an apodizing function causes.
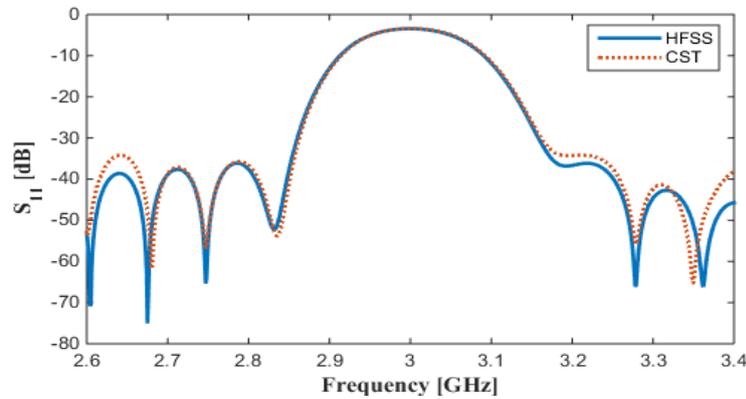

Fig. 6. Reflection coefficient for rectangular waveguide with non-uniform corrugation of Gaussian profile for $\alpha=1$, $\theta=\pi$, and $\delta=0.03a$
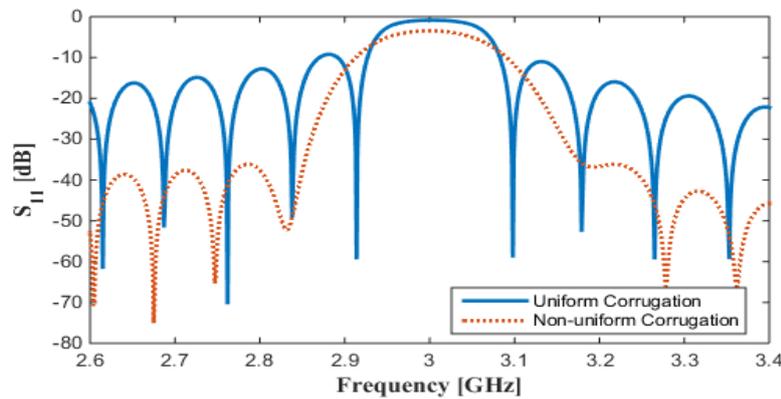

Fig. 7. Reflection coefficient comparison for rectangular waveguide with uniform and non-uniform corrugation for $\alpha=1$, $\theta=\pi$, and $\delta=0.03a$

B) Rectangular Waveguide with Square Corrugations Profile

For a rectangular waveguide whose lateral walls are corrugated as a square wave is shown in Fig. 8, which is governed by Helmholtz's equation:

$$\nabla^2\psi + k_0{}^2\psi = 0 \tag{20}$$

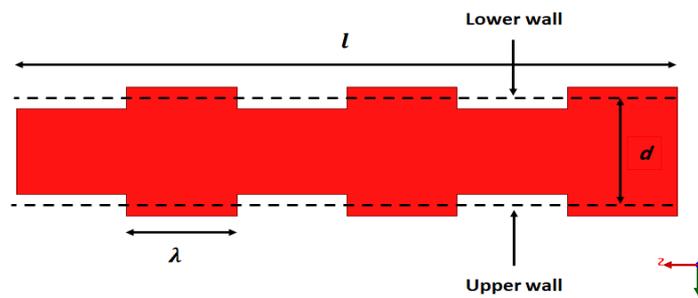where k_0 is the free-space wavenumber; and ψ is the field component.

Fig. 8. Top-view for a rectangular waveguide of square wave corrugation

The boundary conditions are:

$$\frac{\partial^2 \psi}{\partial z^2} + k_0{}^2 \psi = -\frac{\partial^2 \psi}{\partial x \partial z} f'_l(z) \quad \text{at the lower wall } (x = f_l(z)) \tag{21}$$

$$\frac{\partial^2 \psi}{\partial z^2} + k_0{}^2 \psi = -\frac{\partial^2 \psi}{\partial x \partial z} f'_u(z) \quad \text{at the upper wall } (x = 1 + f_u(z)) \tag{22}$$

where $f'_{l(u)}(z)$ denotes the derivative of the wall corrugation function. Corrugation functions are taken as square waves of amplitude $C \ll d$ having a Fourier expansion:

$$f_l(z) = \delta \alpha \sum_{m=1,3,5,\dots} \frac{1}{m} sin(m(kz - \theta)) \tag{23}$$

$$f_u(z) = \delta \sum_{m=1,3,5,\dots} \frac{1}{m} sin(mkz) \tag{24}$$

where $k = \frac{2\pi}{\lambda}$; and λ is the spatial period of the corrugation; $\delta = \frac{4C}{\pi d}$ is the dimensionless corrugation depth; θ is the phase difference between the corrugation of the two walls; and α is a constant allowing for a different corrugation amplitude at the lower plate.

Fig. 9 shows the power reflection coefficient response for the square wave corrugated rectangular waveguide. Fig. 9 clearly shows a multi stop-band.
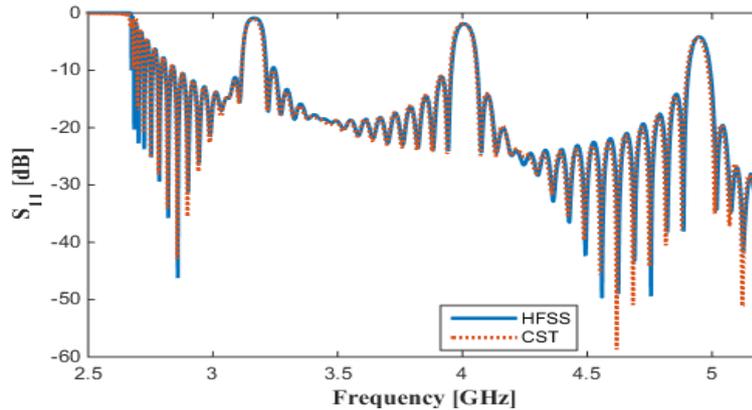

Fig. 9. Reflection coefficient for a rectangular waveguide with square wave corrugation for α=1, θ=π, and δ=0.1d

The square wave is formed of infinite harmonics. This could be the reason for having multi stop-band regions in the frequency response. This could explain the single stop-band in the frequency response that rises as a result of applying a sinusoidal wave as shown in Fig. 2. It is considered one of the infinite harmonics forming the square wave.

III. CONCLUSIONS

In this paper, filtering properties for a rectangular waveguide, with uniform sinusoidal and square corrugation, have been investigated. The uniform sinusoidal wave is considered as the dominant harmonic of a square wave, which gives a single stop-band in the frequency response as suggested in Fig. 2. The case of changing the sign of corrugation depth amplitude δ has also been taken into consideration. The result was a narrow pass-band (inverted notch) window in the stop-band filter region. This can be used in frequency demultiplexing. The first concern of this paper was the reduction of the high ripple level. This has been dealt with by introducing an apodization profile, which is a type of non-uniform corrugation. As a result,

the level of the ripples is decreased; and the bandwidth of the stop-band region is broadened. However, the slight weakness in the strength of the reflection, compared to the case of a uniform corrugation, is due to the decrease in the effective corrugation depth amplitude δ. The paper considers multi-bands in the frequency response by changing the corrugated walls into square wave corrugations. The square wave corrugation gives multi stop-band filter regions. These stopbands are corresponding to fundamental and higher harmonics in the square wave.

REFERENCES

[1] A. Nayfeh, *Introduction to Perturbation Technique*, New York: Wiley Interscience, 1981.

[2] M. Holmes, *Introduction to Perturbation Methods*, New York: Springer-Verlag Inc, 1995.

[3] A. Nayfeh, "Parallel-plate waveguide with sinusoidally perturbed boundaries," *Applied Physics*, vol. 45, no. 11, pp. 4797-4800, 1974.

[4] O. Asfar, "Circular waveguide with sinusoidally perturbed walls," *IEEE Transactions on Microwave Theory and Techniques*, vol. 23, no. 9, pp. 728-734, 1975.

[5] O. Asfar. "Stop bands of the first-order Bragg interaction in a parallel-plate waveguide having multiperiodic wall corrugations," *IEEE Transactions on Microwave Theory and Techniques*, vol. 28, no. 11, pp. 1187-1197, 1980.

[6] O. Asfar and A. Nayfeh, "The application of the method of multiple scales to wave propagation in periodic structures," *SIAM Review*, vol. 25, no. 4, pp. 455-480, 1983.

[7] O. Asfar and M. Bataineh, "Band structure of a parallel-plate waveguide filter having phase-shifted square-wave corrugations," *Waves in Random and Complex Media*, vol. 18, no. 3, pp. 361-370, 2008.

[8] O. Asfar and M. Bataineh, "Microwave filter response of nonuniformly corrugated circular waveguide," *Electromagnetic Waves and Applications*, vol. 9, no. 1-2, pp. 127-143, 1995.

[9] O. Asfar, M. Hawwa, M. Bavencoffe, B. Morvan, and J. Lzbicki, "A multiple-scale perturbation approach to mode coupling in periodic plates," *IEEE Transactions on Ultrasonic, Ferroelectrics and Frequency Control*, vol. 60, no. 2, pp. 395-401, 2013.

[10] O. Asfar, M. Bataineh, and M. Hawwa, "Ultrasonic waveguide with square wave surface grating," *IEEE Transactions on Ultrasonic, Ferroelectrics, and Frequency Control*, vol. 57, no. 8, pp. 1797-1803, 2010.

[11] M. Kehn, "Modal of all-walls longitudinally corrugated rectangular waveguides using asymptotic corrugation boundary conditions," *IEEE Transactions on Microwave Theory and Techniques*, vol. 61, no. 11, pp 3821-3837, 2013.

[12] Y. Li, Q. Wang and C. Wang, "Rectangular waveguide band-pass filter with harmonic suppression," *Proceedings of the International Workshop on Microwave and Millimeter Wave Circuits and System Technology*, pp. 251-253, 2013.

[13] F. Teberio, I. Arnedo, J. Percaz, I. Arregui, T. Lopetegi, and M. Laso, "Accurate design of corrugated waveguide low-pass filters using exclusively closed-form expressions," *Proceedings of 47th European Microwave Conference*, pp. 632-635, 2017.

[14] X. Cheng, R. Chakraborty, S. Mishra, V. Pogrebnyak, and J. Whalen, "Observation of geometric resonance in a corrugated waveguide," *PIERS Online*, vol. 6, no. 2, pp. 137-140, 2010.

[15] V. Pogrebnyak, E. Akray, and N. Kucukaltun. "Tunable stopband in the spectrum for a periodically corrugated waveguide," *Proceedings of Asia-Pacific Microwave Conference*, pp. 1-3, 2005.

[16] *High Frequency Structure Simulator (HFSS)* (Version 15) [Computer software]. Canonsburg, Pennsylvania: Ansoft Corporation. http://www.ansoft.com

[17] *CST Microwave Studio* (Version 11) [Computer software]. Framingham, MA: CST- Computer Simulator Technology. http://www.cst.com

[18] C. Balanis, *Antenna Theory and Design*, New York: John Wiley and Sons, 1997.

[19] A. Hattab, *Nonuniform Periodically Corrugated Rectangular Waveguide Microwave Filter* (Unpublished master's thesis). Jordan University of Science and Technology, Jordan, 1994.

[20] O. Asfar. "A novel narrowband waveguide filter," *Proceedings of IEEE Antennas and Propagation Society International Symposium*, pp. 2526-2529, 1997.

[21] I. Al-Hmoud, *Nonuniform Rectangular Metallic Waveguides: Filtering Properties* (Unpublished master's thesis). Yarmouk University, Jordan, 2016.